The EMBO Journal Vol.16 No.16 pp.4797–4805, 1997

Lysine 156 promotes the anomalous proenzyme activity of tPA: X-ray crystal structure of single-chain human tPA

Martin Renatus[1,2], Richard A.Engh[1,3], Milton T.Stubbs[1,4], Robert Huber[1], Stephan Fischer[3], Ulrich Kohnert[3] and Wolfram Bode[1,2]

[1]Max-Planck-Institute of Biochemistry, Department of Structural Research, D-82152 Martinsried and [3]Biochemical Research Center, Boehringer Mannheim GmbH, Nonnenwald 2, D-82372 Penzberg, Germany

[4]Present address: Institute for Pharmaceutical Chemistry, Philipps-University Marburg, Marbacher Weg 6, D-35032 Marburg, Germany

[2]Corresponding authors
e-mail: renatus@biochem.mpg.de; bode@biochem.mpg.de

Tissue type plasminogen activator (tPA) is the physiological initiator of fibrinolysis, activating plasminogen via highly specific proteolysis; plasmin then degrades fibrin with relatively broad specificity. Unlike other chymotrypsin family serine proteinases, tPA is proteolytically active in a single-chain form. This form is also preferred for therapeutic administration of tPA in cases of acute myocardial infarction. The proteolytic cleavage which activates most other chymotrypsin family serine proteinases increases the catalytic efficiency of tPA only 5- to 10-fold. The X-ray crystal structure of the catalytic domain of recombinant human single-chain tPA shows that Lys156 forms a salt bridge with Asp194, promoting an active conformation in the single-chain form. Comparisons with the structures of other serine proteinases that also possess Lys156, such as trypsin, factor Xa and human urokinase plasminogen activator (uPA), identify a set of secondary interactions which are required for Lys156 to fulfil this activating role. These findings help explain the anomalous single-chain activity of tPA and may suggest strategies for design of new therapeutic plasminogen activators.

Keywords: activation/crystal structure/fibrinolysis/plasminogen activator/zymogen

Introduction

The chymotrypsin family serine proteinases normally are secreted as single-chain zymogens with weak reactivity towards unspecific active site reagents (such as DFP or NPGB) and virtually no reactivity towards peptidic inhibitors such as peptidyl chloromethylketones (Robinson *et al.*, 1973; Morgan *et al.*, 1974; Kerr *et al.*, 1975). They are activated by proteolytic liberation of a highly conserved N-terminus (typically with the sequence IVGG at residues 16–19 in chymotrypsinogen numbering, which is used for tPA throughout this publication; see Table I and Lamba *et al.*, 1996). The free α-amino group forms a solvent-inaccessible salt bridge with the Asp194 carboxylate group in the 'activation pocket' or 'Ile16 cleft' specific for the Ile–Val sequence. The formation of the salt bridge creates a functional substrate recognition site by reorienting Asp194 compared with the proenzyme structure. This reorientation restructures the surrounding activation domain, which includes the oxyanion hole, the catalytic triad and the S1 specificity pocket (Freer *et al.*, 1970; Bode *et al.*, 1976; Fehlhammer *et al.*, 1977; Huber and Bode, 1978). The consequent low and high activities of the zymogen and the cleaved forms, respectively, enabled the evolution of robust regulation of critical biological processes in higher organisms, especially via activation cascades such as found in blood coagulation. Despite the common activation mechanism, the chymotrypsin family proteinases are highly specific for substrates and inhibitors.

Exogenous substances, such as the free dipeptide Ile–Val, can activate the zymogen without proteolytic cleavage. The Ile–Val dipeptide binds in the Ile16 pocket and mimics the activating N-terminus (Bode and Huber, 1976; Bode, 1979). Interactions with very tight binding inhibitors can also induce the formation of an active conformation, as seen for example in the complex of bovine pancreatic trypsin inhibitor (BPTI) with trypsinogen (Bode *et al.*, 1978). Many properties of the single-chain proenzyme form are adequately described by a two-state model: an inactive conformation or set of conformations is in equilibrium with active forms that possess a structured activation domain (Huber and Bode, 1978; Bode, 1979; Coletta *et al.*, 1990). The partition between active and inactive forms depends on environmental conditions, such as the presence of the Ile–Val dipeptide (Bode, 1979), the Ile16 N-terminus (Hedstrom *et al.*, 1996) or other ligands at the substrate-binding site (Bode *et al.*, 1978; Bolognesi *et al.*, 1982). More detailed analyses of the activation of trypsinogen to β-trypsin indicated the presence of several distinguishable activation levels in the transition from zymogen to active enzyme (Coletta *et al.*, 1990). Several crystal structures of serine proteinases and their cognate zymogen forms in different environments are known, most notably chymotrypsin/chymotrypsinogen (Freer *et al.*, 1970; Birktoft and Blow, 1972; Wang *et al.*, 1985) and trypsin/trypsinogen (Bode *et al.*, 1976; Fehlhammer *et al.*, 1977; Huber and Bode, 1978; Bode, 1979).

Tissue type plasminogen activator (tPA) is a chymotrypsin family serine proteinase central to fibrinolysis (for review, see Madison, 1994). It selectively activates the zymogen plasminogen to plasmin by the activation cleavage described above. Plasmin then degrades fibrin with relatively broad specificity and also activates single-chain tPA (sc-tPA); the latter process closes a positive feedback cycle. Plasminogen activation by tPA is strongly stimulated in the presence of fibrin and is inhibited principally by the fast-acting serpin plasminogen activator inhibitor 1

Table I. Important residues cited in this study: residues in chymotrypsinogen numbering and the tPA numbering system

Chymotrypsinogen numbering	tPA numbering
Cys1	Cys264
Gln10	Gln273
Arg15	Arg275
Ile16	Ile276
Lys17	Lys277
Phe21	Phe281
His37	His297
His57	His322
Tyr99	Tyr368
Ser110	Ser379
Lys143	Lys416
His144	His417
Lys156	Lys429
Arg174	Arg449
Thr186	Thr461
Asp194	Asp477
Ser195	Ser478
Ser214	Ser497
Lys222	Lys505
Pro244	Pro527

(PAI-1). It is similar in many ways to uPA (urokinase plasminogen activator), with similar substrate and inhibitor specificities, sequence, structure and function. In contrast to tPA, uPA is found mainly in tissues where it seems to initiate the plasmin-mediated proteolysis of extracellular matrix proteins. Despite their functional and structural similarity, the activities of the single-chain forms of uPA and tPA differ significantly.

In contrast to uPA and other serine proteinases, sc-tPA has significant activity toward small substrates compared with the two-chain form (tc-tPA): it has low 'zymogenicity'. The 'zymogenicity' of a serine proteinase designates the extent of activation upon cleavage, or in other words the ratio of the catalytic activities of the two- and single-chain forms. The low zymogenicity of tPA (5–10: Rånby *et al.*, 1982; Tate *et al.*, 1987; Madison *et al.*, 1993) is in stark contrast to the high zymogenicity of trypsin/trypsinogen (10^7: Bode, 1979). Other serine proteinases have intermediate zymogenicities, such as factor XIIa and urokinase with values of 4000 and 250 (Silverberg and Kaplan, 1982; Lijnen *et al.*, 1990), respectively. The structural basis for these differences, and in particular for the low zymogenicity of tPA, has been unclear, although several factors have been identified. For example, chymotrypsinogen and trypsinogen possess a 'zymogen triad' Asp194–His40–Ser32, which stabilizes Asp194 and the activation domain in a non-functional conformation (Bode, 1979; Madison *et al.*, 1993). These stabilizing factors are absent in tPA and many other serine proteinases. To explain the anomalously low zymogenicity of tPA, salt bridge interactions between Asp194 and one of several lysine residues have been proposed; Lys17 (for tPA numbering see Table I) (Wallén *et al.*, 1983), Lys143 (Petersen *et al.*, 1990) and Lys156 (Nienaber *et al.*, 1992; Lamba *et al.*, 1996; Tachias and Madison, 1997) appeared most likely from model considerations.

Understanding the unusual activity levels of tPA is complicated by the co-factor interactions of fibrin binding. Full-length human tPA, like its physiological substrate plasminogen, binds to fibrin via interactions with the finger domain. In the presence of fibrin, plasmin cleavage by both the sc-tPA and the activated two-chain form is stimulated such that the efficiencies of both forms are similar. In comparison, the catalytic efficiency of tPA's amidolytic activity against chromogenic substrates is stimulated only weakly in the presence of fibrin (Bringmann *et al.*, 1995). This suggests that fibrin stimulation properties occur via a combination of several mechanisms: (i) a major effect by promoting tPA and plasminogen interaction through locally increased concentrations (Hoylaerts *et al.*, 1982; Higgins *et al.*, 1990); (ii) a major effect by promoting suitable orientations and accessibility of the plasminogen substrate cleavage site (Hoylaerts *et al.*, 1982; Lamba *et al.*, 1996); and (iii) an effect promoting the amidolytic efficiency of tPA itself. The latter effect is small [a factor of 4 for human tPA (Bringmann *et al.*, 1995)] but presumably arises from suitable effects in the catalytic domain, slightly altering the catalytic state of the molecule.

We have determined the crystal structure of the catalytic domain of recombinant human sc-tPA in a covalent complex with dansyl-Glu-Gly-Arg-chloromethylketone inhibitor. The structure reveals that the Lys156 side chain is bound in the Ile16 pocket and forms an asymmetric salt bridge with Asp194 (see Figures 2 and 3). Asp194, the active site and the substrate recognition sites are arranged as in tc-tPA (Lamba *et al.*, 1996). This provides evidence that Lys156 plays a role in a non-proteolytic, self-activating process in sc-tPA, leading to its low zymogenicity. A comparison of the sc-tPA structure with other serine proteinase structures also provides a rationale for the higher zymogenicities of other serine proteinases which also have a lysine residue at position 156 but lack the necessary residues in the surrounding environment. Kinetic data confirming the role of Lys156 in the catalytic efficiency of full-length tPA have been published very recently by Tachias and Madison (1997).

Results

Overall structure

The overall three-dimensional structures of the catalytic domain of human tc-tPA in complex with benzamidine (Lamba *et al.*, 1996) and with a bis-benzamidine inhibitor (Renatus,M., Bode,W., Huber,R., Stürzebecher,J., Parsa,D., Fischer,S., Kohnert,U. and Stubbs,M.T., submitted), called here tc-tPA(b) and tc-tPA(bisb) respectively, correspond to that of sc-tPA. Optimal superposition of the sc-tPA and tc-tPA main chains excluding mobile or poorly defined regions (Ser7–Arg15, Lys36–Arg37D, Arg110D, Ser186B–Ala186G, Pro244) and using a distance cutoff of 1.5 Å identifies 238 equivalent Cα positions. The main differences are found in the activation domain (Bode *et al.*, 1976; Huber and Bode, 1978) and in the adjacent surface loops. The catalytic domain of sc-tPA is roughly spherical, with a radius of 25 Å (see Figure 1). The 17 residues of the nominal A chain (residues N-terminal to the cleavage site Arg15–Ile16 of tPA) and the 252 residues of the nominal B chain are continuously linked and, with a few exceptions described below, ordered in the crystal. As in all chymotrypsin family serine proteinases, the molecule consists of two six-stranded barrel-like sub-domains; these pack against each other at an interface which forms

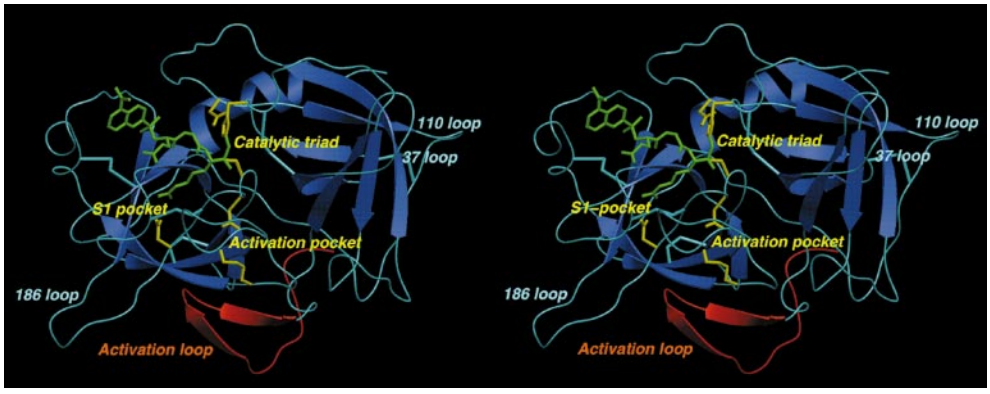

Fig. 1. Stereo ribbon plot of the catalytic domain of sc-tPA in 'standard' orientation. The inhibitor (dansyl-Glu-Gly-Arg-chloromethylketone) shown by green sticks is covalently bonded to Ser195 and His57 of the catalytic triad. Key sc-tPA residues are shown as yellow sticks: Asp102, His57 and Ser195 of the catalytic triad; Asp189 at the base of the S1 specificity pocket; and Asp194 and Lys156 which form a salt bridge in the activation pocket. The red ribbon shows the conformation of the N-terminal activation loop which includes the plasmin cleavage site. Some loops arranged around the active site are labelled: the mainly disordered 37 loop and the 110 loop to the east; the partially disordered 186 loop to the south-west is in proximity to the activation loop. The figure was made with SETOR (Evans, 1993).

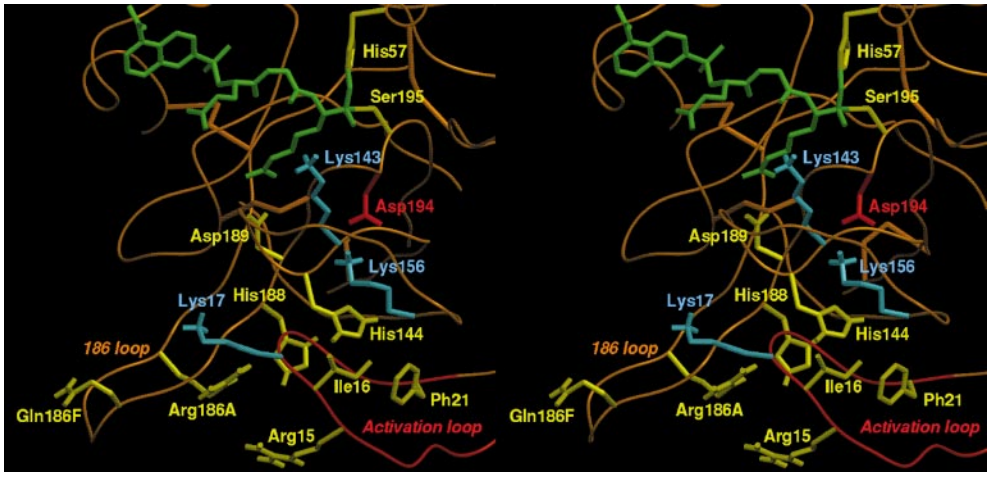

Fig. 2. Stereo plot of the activation domain environment of sc-tPA involving residues of the activation pocket, the activation loop and Lys156. Lys156 (blue) stabilizes the active conformation of sc-tPA via formation of a salt bridge with Asp194 (red). The strength of this interaction is presumably increased by the concerted solvent shielding effect of the (red) activation loop and of the hydrophobic residues Ile16, Phe21 and His144 (yellow). Lysines 17 and 143, which were considered potential activators of sc-tPA (Wallén *et al.*, 1983; Petersen *et al.*, 1990) are also shown (blue). Residues His188, Arg186A and Asn186F of the 186 loop (yellow) are presumed to be responsible for the conformational stabilization of this loop.

the catalytic site. Although the two molecules in the asymmetric unit are not crystallographically identical, no notable differences between them were observed.

Many of the features specific to tPA involve interactions with surface elements and loops of the catalytic domain (Lamba *et al.*, 1996). Since tPA is active in its single-chain form, the comparison of these loops with the two-chain structure is particularly relevant to zymogenicity and the unique aspects of single-chain activity.

The 37 insertion loop points away from the molecular surface into the solvent (to the 'east' of the active site cleft in Figure 1). As in both tc-tPA structures (Lamba *et al.*, 1996), this insertion is only partially defined in the electron density map. No electron density is observed for the six residues Lys36, His37, Arg37A, Arg37B, Ser37C and Pro37D. Although this loop is in the vicinity of a symmetry-related molecule, apparently no specific interactions exist to stabilize a single conformation. This loop has been shown to be of fundamental importance for the interaction with its inhibitor PAI-1 (Madison *et al.*, 1989, 1990a,b) and for fibrin specificity and stimulation (Bennett *et al.*, 1991; Paoni *et al.*, 1993b). The loop flexibility in tPA (and also in uPA, Spraggon *et al.*, 1995) is probably associated with induced conformational changes upon interaction with PAI-1.

The 186 loop, 'south-west' of the active site cleft, contains an insertion of eight residues compared with α-chymotrypsin. The open and extended loop protrudes away from the molecular surface into the solvent. It is bounded on its eastern side (orientation of Figure 2) by the 'activation loop' (see below). Excepting Arg186A and His188, which pair on the molecular surface and approach Arg15 (see Figure 3), and Asn186H, whose Nδ2 is linked with the carbonyl atoms of Ile16 and Gly18, the side chains of this loop do not make stabilizing interactions with other residues on the molecular surface. Part of the loop (Arg186A–Gly186C) is close to a symmetry-related molecule, but also for this near approach neither hydrogen bonds nor hydrophobic interactions were evident. In the conformation of sc-tPA, the 186 loop is close to the entrance frame of the S1 pocket (Ser214–Gln221A) and the turn formed by the succeeding residues Lys222,

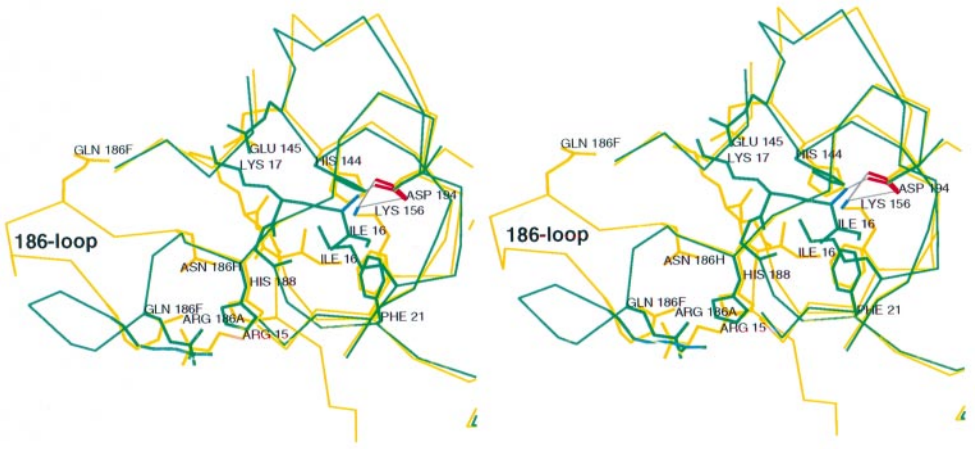

Fig. 3. Superposition of the activation domains of sc-tPA (yellow) and tc-tPA(bisb) (green) (Renatus,M., Bode,W., Huber,R., Stürzebecher,J., Parsa,D., Fischer,S., Kohnert,U. and Stubbs,M.T., submitted). The activation domains are identically formed although the mechanisms by which the active enzyme conformations are achieved (i.e. salt bridge formation with Asp194) differ. The 'active' conformation of Asp194 is stabilized by Lys156 of sc-tPA, but by the N-terminal primary ammonium group of Ile16 in tc-tPA. In the two-chain form, the aliphatic part of the Lys156 side chain is packed between side chains of Ile16, His144 and Phe21, while its distal ammonium group is anchored via hydrogen bonds to Ile16 O and Gly18 O; the first three N-terminal residues Ile16, Lys17 and Gly18 of the B chain are part of a three-strand β-sheet including the segments Lys143–His144 and Asp189–Ala190 (Lamba *et al.*, 1996). In the single-chain form, the activation pocket is shielded from the solvent by the activation loop, in particular through the side chains of residues Ile16 and Phe21, and by the His144 side chain rendering the the salt bridge Lys156Nζ–Asp194Oδ more stable; the activation loop is further fixed in its position by the interaction between the side chains of Lys17 and Glu145. The 186 loop is shifted in sc-tPA relative to the position seen in tc-tPA(bisb), with residues Arg186A, Gln186F and His188 its stabilization.

Asp223 and Val224. The importance of this loop for general function is not clear, since position 186G is deleted in mouse and rat tPA. This region seems to be involved in fibrin stimulation properties (Paoni *et al.*, 1993a); this might, however, be species specific.

The entire 186 loop was defined in tc-tPA(bisb), disordered in tc-tPA(b) (Lamba *et al.*, 1996) and disordered at Gly186C, Gly186D and Pro186E in sc-tPA. Crystal contacts between the 186 loop and a symmetry-related neighbour might account for the order of the loop in tc-tPA(bisb). The density for the ordered residues of the 186 loop in sc-tPA shows that the loop is shifted relative to the position seen in tc-tPA(bisb), although the backbone conformations are similar where they are ordered (an approximate hinge position is evident in Figure 3). The crystal packing of the sc-tPA structure does not exclude the conformation of the 186 loop seen in tc-tPA(bisb). Also, the differing conformation of the adjacent 'activation loop' in sc-tPA (see below) would not obviously exclude the conformation of the 186 loop in tc-tPA(bisb) (see Figure 3). Different pH levels in the crystals may contribute to differences in the loop structure. The tc-tPA(b) crystals were grown at pH 7.3 (Lamba *et al.*, 1996), the tc-tPA(bisb) crystals at pH 5.0 and the sc-tPA crystals at pH 7.2. For the tc-tPA(bisb) structure, the stabilization of the 186-loop in its particular conformation was attributed to a cluster of three residues: Arg186A, Gln186F and especially His188, whose protonation state presumably varies in the pH range.

The 'autolysis' loop, Tyr141–Tyr151, located to the south of the active site cleft, is well defined by electron density. As in tc-tPA, the hydrophobic residues Leu147, Pro149 and Phe150 are exposed to the solvent, suggesting that this region might participate in specific interactions with substrates, inhibitors and co-factors (Lamba *et al.*, 1996; Ke *et al.*, 1997). The side chain of Tyr151 extends into the S2′ subsite. The side chain of Glu145 forms a salt bridge with Nζ Lys17 in tc-tPA(bisb) and in sc-tPA, although the Cα position of Lys17 is quite different in both cases.

Insertion loops 186 and 110 (characteristic for plasminogen activators) lie approximately on the long axis of the catalytic domain and at opposite poles (Figure 1). Although the 110 insertion loop is completely defined in tc-tPA(b), the single residue Arg110D is undefined in sc-tPA. In tc-tPA(bisb), the three residues Asp110A, Ser110B and Ser110C are undefined; the equivalent insertion loop of uPA (Spraggon *et al.*, 1995) shows high mobility. Thus this loop may be flexible under physiological conditions. No hypothesis about its function has been reported so far. The last residue at the C-terminus, Pro244, and the side chain of Arg243, which are close to the '110 loop', are also undefined in sc-tPA.

N-terminal segment, activation loop and Ile16 cleft

In the hemisphere opposite to that of the active site cleft, the N-terminal segment of the catalytic domain of human tPA is linked to the rest of the molecule by the disulfide Cys1–Cys122. In the structure reported here, it comprises the first three N-terminal residues Ser1E–Tyr1D–Gln1C of the full-length tPA, the two residues Ser1B and Thr1A of the linker between kringle 2 and the catalytic domain, and the initial part of the activation peptide (Cys1–Arg15). The 'activation loop' comprises residues Gln10–Phe21, including the activation cleavage site Arg15–Ile16 (see Figures 2 and 3). Residues Cys1–Lys17 follow the molecular surface in an almost extended conformation, forming a short antiparallel β-sheet with inter-main chain hydrogen bonds (Gln10N...Phe21O, Phe11O...Phe21N, Ile16N... Gly19O, Ile16O...Gly19N). Segment Ile16–Lys17–Gly18–Gly19 forms an almost regular 1,4-tight turn (Figures 2 and 3).

As in the crystal structure of the catalytic domain of tc-tPA, the first four N-terminal residues (Ser1E–Tyr1D–Gln1C–Ser1B) of the nominal A chain are not defined by

electron density. From Thr1A upstream, almost all main chain atoms of the A chain (with the exception of Gly2) and all side chain atoms (with the exceptions of Gln8 and Gln10) are defined by electron density. The geometry of the residues from Thr1A to Gln5 are very similar to the corresponding residues of tc-tPA, with Arg4 and Glu137 forming a salt bridge. Carboxy-terminal to Tyr6, the polypeptide chain in sc-tPA follows the molecular surface, while in tc-tPA the corresponding part of the A chain is not defined by electron density and might point into the solvent.

Ile16, Phe21 and His144 form a hydrophobic cluster and partially shield the Ile16 cleft from solvent (see Figures 2 and 3). Several residues of the Ile16–Gly19 turn segment form additional stabilizing interactions with the adjacent autolysis and 186 surface loops: the carbonyl oxygen of Ile16 forms a hydrogen bond with the $N\delta_2$ of Asn186H, $N\zeta$ of Lys17 with $O\varepsilon_1$ of Glu145 and the carbonyl oxygen of Gly18 with N of Asp189. Glu144 is stabilized further by an interaction with the carbonyl oxygen of Cys220. The net effect of these interactions is to stabilize the 'activation loop' segment Phe11–Leu20 in a conformation resembling a flap or lid which shields the Ile16 pocket and the salt bridge Lys156–Asp194 from solvent.

The Lys156–Asp194 salt bridge interaction confirms the hypothesis (Nienaber *et al.*, 1992; Lamba *et al.*, 1996) that Lys156 is particularly important for the low zymogenicity of tPA, which has now been supported by mutagenesis studies (Tachias and Madison, 1997). The side chains of Lys17 (Wallén *et al.*, 1983) and Lys143 (Petersen *et al.*, 1990), other candidates hypothesized to form the decisive salt bridge interaction with Asp194, extend away from the Ile16 pocket and are exposed to the bulk solvent; Lys17Nζ forms a salt bridge with Glu145Oε. The Ile16 pocket is shielded by the activation turn (Ile16–Gly19) and the hydrophobic cluster of Ile16, Phe21 and His144. Both shielding elements presumably increase the strength of the salt bridge interaction and may be an additional requirement for single-chain activity (see below for a discussion of single-chain activity relative to other Lys156-containing serine proteinases). The shielding position of the 'activation loop' is stabilized by: (i) hydrophobic interactions (between Ile16 and the aromatic groups of Phe11, Phe21 and Phe150); (ii) the formation of a salt bridge between Lys17 and Glu145 (Glu145 $O\varepsilon_2$ makes a further interaction with Cys220 O); and (iii) the hydrogen bonds Asn186HNδ...Ile16O and Gly18O...Asp189N.

By comparison, the tc-tPA structures are identical to sc-tPA for main chain atoms C-terminal to Leu20 and, as described above, N-terminal to Gln5. N-terminal to Leu20, the main chain of tc-tPA changes its direction abruptly at residues Gly18 and Gly19 (ψ-Gly18: –144° in tc-tPA and –21° in sc-tPA, ϕ-Gly19: 68° in tc-tPA and 177° in sc-tPA, see Figure 3). Consistent with their conservation among serine proteinases, Gly18 and Gly19 possess the flexibility required upon activation cleavage to allow Ile16 to insert into the Ile16 pocket and to form the internal salt bridge with Asp194. Lys156 adopts a g^+-rotamer conformation in tc-tPA and a g^--rotamer conformation in sc-tPA. The side chain of Lys156 in tc-tPA is exposed to solvent and forms hydrogen bonds with carbonyl oxygen atoms of the activation peptide at Gly18 and Gly17 (see Figure 3).

Inhibitor binding

The inhibitor molecule as bound into the functional active site of sc-tPA is shown in Figure 4. The continuous density indicates the two covalent bonds between the P1 Arg group (residue ArmI3) and the enzyme, as is known from other serine proteinase structures complexed with chloromethylketone inhibitors (Bode *et al.*, 1992; Brandstetter *et al.*, 1995; Spraggon *et al.*, 1995; Mather *et al.*, 1996). The bonds exist between His57Nε_2 and the methylene carbon and between Ser195Oγ and the carbonyl carbon, representing a tetrahedral hemiketal structure (Powers, 1977).

The inhibitor backbone abuts the segment Ser214–Gly217, forming a short antiparallel slightly twisted β-sheet interaction. The side chain of ArmI3 binds in the S1 pocket, forming symmetric twin salt bridges between $N\eta_1/N\eta_2$ and $O\delta_1/O\delta_2$ of Asp189 at the bottom of the pocket. $N\eta_1$ forms an additional hydrogen bond to the carbonyl oxygen of Gly219 (d = 2.7 Å), as seen for substrate analogues containing an Arg at P1 as well as amidine-derived inhibitors in complex with serine proteinases. GlyI2 occupies the rather small S2 pocket of tPA and approaches the Oη group of Tyr99. This is consistent with the tPA preference for Gly as a substrate P2 residue (Ding *et al.*, 1995; Madison *et al.*, 1995). The side chain of GluI1 forms weak hydrogen bonds with the N of Gly219 and with the side chain of Gln192. The GluI1 carbonyl oxygen forms a favourable hydrogen bond with N Gly216. GluI1 and the dansyl group are also involved in crystal contacts. The N-terminus of the inhibitor is masked with a dansyl group. Although this group, with its combined aromatic moiety and distal amine, might be considered an ideal S4 binding group for tPA (Renatus,M., Bode,W., Huber,R., Stürzebecher,J., Parsa,D., Fischer,S., Kohnert,U. and Stubbs,M.T., submitted; see also the related discussion for factor Xa, Brandstetter *et al.*, 1996), it does not bind into the hydrophobic S3/S4 cleft of tPA (Lamba *et al.*, 1996), maybe due to steric hindrance caused by the dimethyl moieties. Rather, the group binds in an aromatic depression in a symmetry-related neighbour formed by residues Thr186, Tyr163, Trp133, Arg167 and Asp223. As with loop conformations, this binding geometry may determine crystal packing, or, conversely, the crystal packing interactions may have influenced the inhibitor binding interactions.

Discussion

The crystal structure described here contributes to a detailed understanding of the unique properties of sc-tPA compared with the two-chain form and compared with other chymotrypsin family serine proteinases. The most prominent of these features is the high catalytic efficiency prior to activation cleavage or, equivalently, the low zymogenicity of tPA. As described in the Introduction, the zymogenicity of the single-chain molecule is roughly described by a two-state model consisting of an inactive form in equilibrium with an active form which possesses a structured activation domain. In serine proteinases with

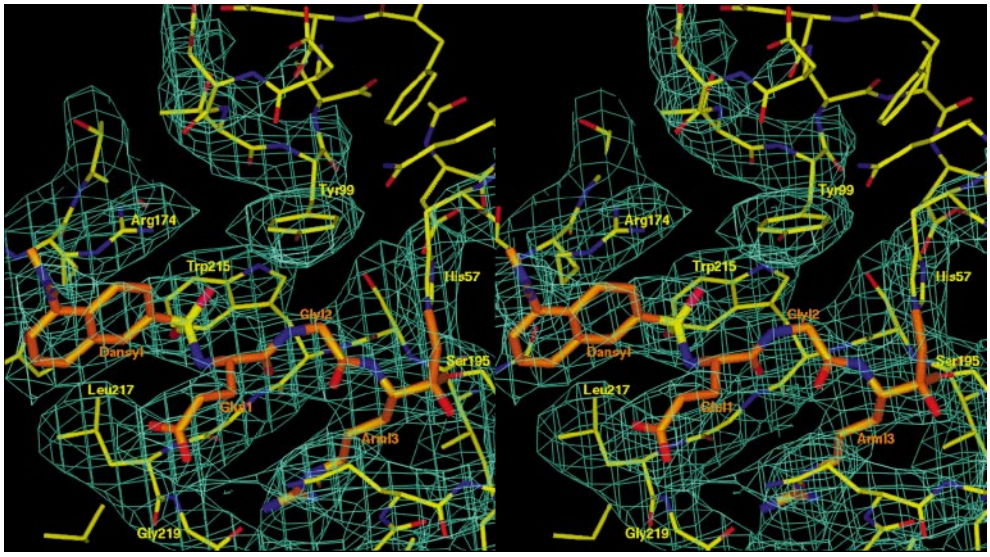

Fig. 4. Dansyl-Glu-Gly-Arg-chloromethylketone inhibitor (orange) and part of the active site of sc-tPA (yellow) superimposed on the final $2F_o–F_c$ electron density contoured at 0.9σ, oriented as in Figure 1. The figure was made with Main (Turk, 1992).

high zymogenicity, such as trypsin, the equilibrium can be shifted toward the active form only by such environmental factors as extremely tight binding inhibitors [BPTI and porcine pancreatic secretory inhibitor (PSTI)] or high concentrations of an activating ligand (Ile–Val). In tPA, amidolytic activity with respect to chloromethylketone inhibitors suggests that a significant population of tPA is pre-formed with an active conformation in the absence of such environmental factors (Powers, 1977). As described above, the structure shows that Lys156 forms a stabilizing salt bridge with Asp194 in an active conformation. This may lower the energy difference between active and inactive states sufficiently to allow a residual population of active states and generate the observed low zymogenicity. The energy of inhibitor binding would then be sufficient to shift the equilibrium fully to the active conformation, as observed in the crystal structure.

Lys156 is not unique to tPA among chymotrypsin family serine proteinases and, taken alone, does not offer an adequate explanation for the uniquely low zymogenicity of tPA. The four tPA sequences determined to date (human, rat, mouse and vampire bat) possess a lysine residue at position 156; Lys156 also is found conserved in other serine proteinases with low single-chain activity. Thus, Lys156 is not solely responsible for the high activity of sc-tPA, but rather acquires this function through secondary interactions made apparent by comparison with crystal structures of other serine proteinases. These interactions seem to be provided mainly by residues 21 and 144 and by the activation loop.

Approximately one-seventh of 209 chymotrypsin-like serine proteinase sequences with at least 30% identity (EMBL Predict Protein server, August 1996) to the catalytic domain of human tPA have a lysine residue at position 156. These include bovine trypsinogen, plasminogen, blood clotting factor X and uPA, enzymes with zymogenicities much higher than tPA. Arginine and histidine also appear relatively frequently at this position (43/209 and 7/209, respectively) and might also be considered candidates for intramolecular zymogen activation properties analogous to those of Lys156. Lysine is conserved at position 156 in all urokinase sequences determined to date (baboon, human, pig, bovine, rat and mouse) except that of chicken. Plasminogen sequences (dog, rhesus macaque, mouse, horse, human, cow and pig) show a strict conservation of Lys156. Some factor X (human), factor IX and trypsin (bovine) sequences also contain Lys156, although the degree of conservation is less than that of the fibrinolytic factors.

Comparisons of the relevant serine proteinase structures [the zymogen structures sc-tPA, vampire bat PA (Renatus,M., Stubbs,M.T., Huber,R., Bringmann,P., Schlenning,W.-D. and Bode,W., submitted) and bovine trypsinogen (Fehlhammer *et al.*, 1977; Bode *et al.*, 1978; Bolognesi *et al.*, 1982), and several activated proteinases, such as tc-tPA (Lamba *et al.*, 1996), uPA (Spraggon *et al.*, 1995), factor Xa (Padmanabhan *et al.*, 1993; Brandstetter *et al.*, 1996), factor IXa (Brandstetter *et al.*, 1995) and bovine trypsin] suggests a critical role for residues 21 and 144 in determining the activating potential of Lys156. The crystal structure of human two-chain uPA shows Glu144 to form a salt bridge with Lys156 at the protein surface away from the Ile16 pocket (Spraggon *et al.*, 1995), presumably an energetically favourable alternative to Asp194 also in the sc-uPA form. Chicken uPA, interestingly, possesses Met156 and Gln144; the simultaneous loss of a potentially activating lysine at position 156 and a salt bridge partner at 144 is consistent with a hypothetical need for uPA to prevent zymogen activity. The crystal structure of inhibitor-bound human factor Xa shows Lys156 hydrogen-bonded to Thr144 away from the Ile16 pocket (Brandstetter *et al.*, 1996), similar to the structure in uPA. In bovine trypsinogen, in the bovine trypsinogen–BPTI complex and in bovine β-trypsin, the Lys156 Nζ forms a hydrogen bond with the Oγ of Thr21. Thus alcohol or acid groups at positions 21 and 144 may compete with a zymogen-activating Asp194–Lys156 salt bridge. This hypothesis is corroborated by recent mutant studies by Tachias and Madison (1996).

Only three structures hitherto described show the

formation of a salt bridge between Lys156 and Asp194: the catalytic domain of sc-tPA presented here, the catalytic domain of vampire bat PA, which exists only as a single-chain molecule (Gardell *et al.*, 1989), and PSTI–trypsinogen complex (Bolognesi *et al.*, 1982). The sc-tPA structures are consistent with their high proteolytic activity. The tPA sequences available to date show that neither residue 21 nor residue 144 offer interactions to compete with Asp194–Lys156 bridge formation: residue 21 has an aromatic side chain (Phe in human, rat and bat; Tyr in mouse tPA), while residue 144 is in all cases a His, which under physiological conditions will probably be at least partially protonated and electrostatically repulsive to Lys156. Besides tPA, the only sequences which simultaneously have lysine at position 156 but have neither an alcoholic nor an acidic amino acid at positions 21 or 144 are found for two granzymes [human granzyme A precursor (Gershenfeld *et al.*, 1988) and mouse granzyme D precursor (Jenne *et al.*, 1988)] and human complement C1r precursor (Leytus *et al.*, 1986). The granzymes are apparently processed in the cell, and little is known about their single-chain properties. C1r occurs only in a single-chain form and is believed to be activated not by proteolytic processing but by binding to its co-factor C1q; here also, Lys156 might assist in gaining activity before activation cleavage.

The occurrence of the salt bridge Lys156–Asp194 in the structure of the trypsinogen–PSTI complex (Bolognesi *et al.*, 1982), in spite of the very low activity of trypsinogen, is in apparent contradiction to the rules described above. In the trypsinogen–BPTI complex, no stabilizing interaction is found between Lys156 and Asp194, although the latter side chain is found in the 'active' conformation; instead, Lys156 makes a hydrogen bond with Thr21 as seen in free trypsinogen. This indicates that the salt bridge Lys156–Asp194 is not necessary for the binding of strong inhibitors to trypsinogen. The existence of this salt bridge in the trypsinogen–PSTI complex is probably a result of special secondary interactions between the enzyme and inhibitor: the restructuring of the autolysis loop upon inhibitor binding causes the activation peptide to approach the molecular surface. This renders the activation pocket less accessible to solvent, disallows the hydrogen bond between Thr21 and Lys156 (or the potential favourable interaction between Thr144 and Lys156) and thereby favours the formation of the Lys156–Asp194 salt bridge.

The crystal structure of the sc-tPA catalytic domain thus provides an explanation for the anomalously high activity and low zymogenicity of sc-tPA. In the absence of the fibrin co-factor, the salt bridge formation between Lys156 and Asp194 apparently plays a key role in stabilizing the active conformation of sc-tPA. Mutagenesis studies also confirm an important role; Lys156→Tyr mutants indeed exhibit lower single-chain activity than wild-type enzyme and have, therefore, a substantially enhanced zymogenicity (Tachias and Madison, 1997). For full-length human tPA, fibrin also plays a role: the presence of fibrin increases the amidolytic activity 4-fold and the plasminogenolytic activity by a factor of 550 (Bringmann *et al*., 1995) to 3800 (Tachias and Madison, 1997). This fibrin stimulation can be assigned largely to the assemblage of enzyme and substrate on the fibrin template: plasminogen is probably fixed to the fibrin surface, with its cleavage site oriented to the active site of an adjacent tPA molecule. The catalytic apparatus might be influenced in addition by direct interactions between fibrin attachment sites of the catalytic domain [such as the 'fibrin-binding patch' (Paoni *et al.*, 1993a; Lamba *et al.*, 1996)] and specific anchoring sites on fibrin, supporting the conversion from the inactive to the active zymogen conformation. A detailed understanding of fibrin stimulation requires further structural data on the ternary fibrin–tPA–plasminogen complex.

The properties of full-length tPA arose of course through evolution of fibrinolysis in functional physiological systems. Under pathophysiological conditions, such as myocardial infarction, new functional properties might be important for effective thrombolytic therapy. Recently, it has been shown in a dynamic clot lysis model (U.Kohnert and S.Fischer, in preparation) that N-terminal truncated tPA mutants such as rPA (consisting of kringle 2 and the catalytic domain) exhibit shorter clot perfusion times resulting from the lack of high affinity fibrin binding of the mutant and thus better clot penetration. This effect is also relevant for the catalytic domain of tPA itself (Kohnert *et al.*, 1996). Mutein design with an aim to optimize therapeutic properties, in particular introduction of variations in important regions such as the activation domain, is a promising method towards continued development of new therapeutic plasminogen activators.

Materials and methods

Expression, purification and inhibition of the protein

The des(Val4–Cys261) tPA variant (Pannekoek *et al.*, 1990) was expressed as inclusion bodies in *Escherichia coli*, isolated, refolded and purified on an ETI-Sepharose column as previously described (Kohnert *et al.*, 1996).

The enzyme was inhibited with dansyl-Glu-Gly-Arg-chloromethylketone (Calbiochem). Five µl of a freshly prepared inhibitor solution (100 mM in dimethylsulfoxide) were added to 1 ml of protein solution (c_{prot} = 2.2 mg/ml in 0.5 M phosphate buffer at pH 7.2) and incubated at room temperature for 40 min. The catalytic activity was checked using the chromogenic substrate S2288 (Chromogenix) and was found to be reduced to <0.5% of the initial activity.

Crystallization and structure analysis

Crystals were grown using the sitting-drop vapour-diffusion method. Three µl of the protein (2.8 mg/ml in 10 mM acetate buffer pH 4.5) and 1.5 µl of the reservoir solution (0.1 M acetate buffer pH 7.2, 0.2 M $MgCl_2$, 8% polyethyleneglycol monomethylester 6K, 4% methane pentane diol) were mixed and equilibrated at 23°C against 1 ml of reservoir solution. Bushels of plate-shaped crystals grew within 1 week. Two protein drops containing such crystals were subjected to N-terminal sequencing; a separate sequencing of crystal and mother liquor was impossible due to the fragility of the crystals. More than 90% of the signal detected for the first amino acid was due to the N-terminal Ser1E. Ile was found only in trace amounts, indicating that the inhibited sc-tPA had not undergone proteolytic cleavage during crystal growth. A crystal of $0.2\times0.15\times0.04$ mm^3 was mounted and indexed as belonging to the orthorhombic space group $P2_12_12_1$, with cell constants a = 43.99 Å, b = 80.78 Å, c = 159.16 Å, $\alpha = \beta = \gamma = 90°$. Estimation of the solvent content indicated that the crystals contain two molecules per asymmetric unit with a fractional v/v solvent content of 50% (V_m = 2.4 Å^3/Dalton). Diffraction data to 3.2 Å were collected on a MAR image plate system (MAR Research, Hamburg) mounted on a Rigaku rotating anode X-ray generator and processed using the Mosflm package (Leslie, 1994) (see Table II for crystallographic data). The structure was solved by Patterson search techniques with the program AMoRe (Navaza, 1994), using an integration radius of 30 Å and resolution limits of 15.0–3.5 Å. The search model consisted of the catalytic domain of tc-tPA(b) (Lamba *et al.*, 1996), excluding the '186 loop'. The rotation function gave one peak at 28.3% correlation and 11.4% for the next best angle triplet. The

Table II. Crystal data and refinement parameters for the catalytic domain of human sc-tPA

Space group	$P2_12_12_1$
Cell constants (Å)	
a	43.99
b	80.78
c	156.16
Significant measurements	27 265
Independent reflections	9414
Limiting resolution (Å)	3.1
Completeness	86.1% (∞–3.1Å)
outermost shell	55.2% (3.18–3.1 Å)
R_{merge}[a]	14.7%
outermost shell	63.0% (3.18–3.1Å)
No. of atoms per asymmetric unit	
non-hydrogen protein atoms	4170
non-hydrogen inhibitor atoms	82
solvent molecules	19
Resolution range (Å)	7.0–3.25
Reflections used for refinement	6846
Completeness (2σ cutoff) (%)	85.22
outermost shell	29.20% (3.35–3.25 Å)
R-value[b]	20.37%
r.m.s. standard deviation	
bond lengths (Å)	0.06
bond angles (°)	1.642
RMSB (Å^2)[c]	2.5

[a]$R_{merge} = \Sigma(I-<I>)/\Sigma I$.
[b]$R_{merge} = \Sigma|F_{obs}|-|F_{calc}|/\Sigma|F_{obs}|$.
[c]RMSB: r.m.s. deviation of the *B*-factor of bonded atoms.

translation function corresponding to the highest rotation peak yielded two peaks with different translation vectors (36.6 and 36.0% correlation, 32.2% for next highest peak). After rigid-body refinement of both independent molecules, the correlation and the *R*-factor were 73.7 and 35.1%, respectively.

Conventional crystallographic refinement (rigid-body, positional and temperature factor) was carried out using the parameters of Engh and Huber (1991). In the latter stages of refinement, restrained individual *B*-factor refinement was applied. Except for residues belonging to partially undefined surface loops and residues in the proximity of such regions, all atoms were restrained to obey true non-crystallographic symmetry. Disordered residues (Leu147 of molecule A, Gln10 and Arg110A of molecule B, Lys36–Pro37D, Arg110D Gly186C–Pro186E and Arg243–Pro244 of both independent molecules) and side chains were excluded from phasing but were included in the coordinate set (except the N-terminal residues Ser1E–Ser1B of both independent molecules). Model building was performed using Main (Turk, 1992). Averaging over the non-crystallographic symmetry elements using CCP4 (Collaborative Computional Project No. 4, 1993) provided no significant improvement of the electron density after the third cycle of model bilding. The program PROCHECK (Laskowski *et al.*, 1993) indicates that 72.5% of the residues fall within the most favoured region of the Ramachandran plot, and that no residues are in the 'disallowed regions'. Crystallographic and refinement data are given in Table II. The secondary structure of sc-tPA was calculated with STRIDE (Frishman and Argos, 1995).

Acknowledgements

The financial support of the SFB469, the 'Fonds der Chemischen Industrie' and the EU BIOMED ERB-BMH4-CT96-0937 project is gratefully acknowledged.

References

Bennett,W.F., Paoni,N.F., Keyt,B.A., Botstein,D., Jones,A.J.S., Presta,L., Wurm,F.M. and Zoller,M.J. (1991) High resolution analysis of functional determinants on human tissue-type plasminogen activator. *J. Biol. Chem.*, **266**, 5191–5201.

Birktoft,J.J. and Blow,D.M. (1972) Structure of crystalline α-chymotrypsin. V. The atomic structure of tosyl-α-chymotrypsin at 2 Å resolution. *J. Mol. Biol.*, **68**, 187–240.

Bode,W. (1979) The transition of bovine trypsinogen to a trypsin-like state upon strong ligand binding. II. The binding of the pancreatic trypsin inhibitor and of isoleucine–valine and of sequentially related peptides to trypsinogen and to *p*-guanidinobenzoate-trypsinogen. *J. Mol. Biol.*, **127**, 357–374.

Bode,W. and Huber,R. (1976) Induction of the bovine trypsinogen–trypsin transition by peptides sequentially similar to the N-terminus of trypsin. *FEBS Lett.*, **68**, 231–236.

Bode,W., Fehlhammer,H. and Huber,R. (1976) Crystal structure of bovine trypsinogen at 1.8 Å resolution. I. Data collection, application of Patterson search techniques and preliminary structural interpretation. *J. Mol. Biol.*, **106**, 325–335.

Bode,W., Schwager,P. and Huber,R. (1978) The transition of bovine trypsinogen to a trypsin-like state upon strong ligand binding. The refined crystal structures of the bovine trypsinogen–pancreatic trypsin inhibitor complex and of its ternary complex with Ile–Val at 1.9 Å resolution. *J. Mol. Biol.*, **118**, 99–112.

Bode,W., Turk,D. and Karshikov,A. (1992) The refined 1.9 Å X-ray crystal structure of D-Phe-Pro-Arg chloromethylketone-inhibited human α-thrombin: structure analysis, overall structure, electrostatic properties, detailed active-site geometry, and structure–function relationships. *Protein Sci.*, **1**, 426–471.

Bolognesi,M., Gatti,G., Menegatti,E., Guarneri,M., Marquart,M., Papamokos,E. and Huber,R. (1982) Three-dimensional structure of the complex between panereatic secretory trypsin inhibitor (kazal type) and trypsinogen at 1.8 Å resolution. Structure solution, crystallographic refinement and preliminary interpretation. *J. Mol. Biol.*, **162**, 839–868.

Brandstetter,H., Bauer,M., Huber,R., Lollar,P. and Bode,W. (1995) X-ray structure of clotting factor IXa: active site and module structure related to Xase activity and hemophilia B. *Proc. Natl Acad. Sci. USA*, **92**, 9796–9800.

Brandstetter,H., Kühne,A., Bode,W., Huber,R., von der Saal,W., Wirthensohn,K. and Engh,R.A. (1996) X-ray structure of active site-inhibited clotting factor Xa. Implications for drug design and substrate recognition. *J. Biol. Chem.*, **271**, 29988–29992.

Bringmann,P., Gruber,D., Liese,A., Toschi,L., Krätzschmar,J., Schleuning,W.D. and Donner,P. (1995) Structural features mediating fibrin selectivity of vampire bat plasminogen activators. *J. Biol. Chem.*, **270**, 25596–25603.

Coletta,M., Ascenzi,P., Bravin,L., Amiconi,G., Bolognesi,M., Guarneri,M. and Menegatti,E. (1990) Thermodynamic modeling of internal equilibria involved in the activation of trypsinogen. *J. Biomol. Struct. Dynam.*, **7**, 959–972.

Collaborative Computional Project, No. 4 (1994) The CCP4 suite: programs for protein crystallography. *Acta Crystallogr.*, **D50**, 760–763.

Ding,L., Coombs,G.S., Strandberg,L., Navre,M., Corey,D.R. and Madison,E.L. (1995) Origins of the specificity of tissue-type plasminogen activator. *Proc. Natl Acad. Sci. USA*, **92**, 7627–7631.

Engh,R.A. and Huber,R. (1991) Accurate bond and angle parameters for X-ray protein structure refinement. *Acta Crystallogr.*, **A47**, 392–400.

Evans,S.V. (1993) SETOR: hardware lighted three-dimensional solid model representations of macromolecules. *J. Mol. Graph.*, **11**, 134–138.

Fehlhammer,H., Bode,W. and Huber,R. (1977) Crystal structure of bovine trypsinogen at 1.8 Å resolution. II. Crystallographic refinement, refined crystal structure and comparison with bovine trypsin. *J. Mol. Biol.*, **111**, 415–438.

Freer,S.T., Kraut,J., Robertus,J.D., Wright,H.T. and Xuong,N.H. (1970) Chymotrypsinogen, 2.5 Å crystal structure, comparison with α-chymotrypsinogen and implications for zymogen activation. *Biochemistry*, **9**, 1997–2009.

Frishman,D. and Argos,P. (1995) Knowledge-based secondary structure assignment. *Proteins*, **23**, 566–579.

Gardell,S.J., Duong,L.T., Diehl,R.E., York,J.D., Hare,T.R., Register,R.B., Jacobs,J.W., Dixon,R.A. and Friedman,P.A. (1989) Isolation, characterization, and cDNA cloning of a vampire bat salivary plasminogen activator. *J. Biol. Chem.*, **264**, 17947–17952.

Gershenfeld,H.K., Hershberger,R.J., Shows,T.B. and Weissmann,I.L. (1988) Cloning and chromosomal assignment of a human cDNA encoding a T cell- and natural killer cell-specific trypsin-like serine protease. *Proc. Natl Acad. Sci. USA*, **85**, 1184–1188.

Hedstrom,L., Lin,T.Y. and Fast,W. (1996) Hydrophobic interactions control zymogen activation in the trypsin family of serine proteases. *Biochemistry*, **35**, 4515–4523.

Higgins,D.L., Lamb,M.C., Young,S.L., Powers,D.B. and Anderson,S. (1990) The effect of the one-chain to two-chain conversion in tissue plasminogen activator: characterization of mutations at position 275. *Thromb. Res.*, **57**, 527–539.

Hoylaerts,M., Rijken,D.C., Lijnen,H.R. and Collen,D. (1982) Kinetics of the activation of plasminogen by human tissue plasminogen activator. Role of fibrin. *J. Biol. Chem.*, **257**, 2912–2919.

Huber,R. and Bode,W. (1978) Structural basis of the activation and action of trypsin. *Acc. Chem. Res.*, **11**, 114–122.

Jenne,D., Rey,C., Haefliger,J.-A., Qiao,B.-Y., Groscurth,P. and Tschopp,J. (1988) Identification and sequencing of cDNA clones encoding the granule-associated serine proteases granzymes D, E and F of cytolytic T lymphocytes. *Proc. Natl Acad. Sci. USA*, **85**, 4814–4818.

Ke,S.-H., Lamba,K. Tachias,D., Bode,W. and Madison,E.L. (1997) Identification of a hydrophobic exosite on tissue type plasminogen activator that modulates specificity for plasminogen. *J. Biol. Chem.*, **272**, 1811–1816.

Kerr,M.A., Walsh,K.A. and Neurath,H. (1975) Catalysis by serine proteases and their zymogens. A study of acyl intermediates by circular dichroism. *Biochemistry*, **14**, 5088–5094.

Kohnert,U., Hellerbrand,K., Martin,U., Stern,A., Popp,F. and Fischer,S. (1996) The recombinant *Escherichia coli*-derived protease-domain of tissue-type plasminogen activator is a potent and fibrin specific fibrinolytic agent. *Fibrinolysis*, **10**, 93–102.

Lamba,D., Bauer,M., Huber,R., Fischer,S., Rudolph,R., Kohnert,U. and Bode,W. (1996) The 2.3 Å crystal structure of the catalytic domain of recombinant two-chain human tissue-type plasminogen activator. *J. Mol. Biol.*, **258**, 117–135.

Laskowski,R.A., MacArthur,M.W., Moss,S.D. and Thorton,J.M. (1993) PROCHECK: a programme to check the stereochemical quality of protein structures. *J. Appl. Crystallogr.*, **26**, 283–291.

Leslie,A.G.W. (1994) *Mosflm User Guide, Mosflm Version 5.20*. MRC Laboratory of Molecular Biology, Cambridge, UK.

Leytus,S.P., Kurachi,K., Sakariassen,K.S. and Davie,E.W. (1986) Nucleotide sequence of the cDNA coding for human complement Clr. *Biochemistry*, **25**, 4855–4863.

Lijnen,H.R., Van Hoef,B., Nelles,L. and Collen,D. (1990) Plasminogen activation with single-chain urokinase-type plasminogen activator (scu-PA). Studies with active site mutagenized plasminogen (Ser740→Ala) and plasmin-resistant scu-PA (Lysl58→Glu). *J. Biol. Chem.*, **265**, 5232–5236.

Madison,E.L. (1994) Probing structure–function relationships of tissue-type plasminogen activator site-specific mutagenesis. *Fibrinolysis*, **8**, 221–236.

Madison,E.L., Goldsmith,E.J., Gerard,R.D., Gething,M.-J.H. and Sambrook,J.F. (1989) Serpin-resistant mutants of human tissue-type plasminogen activator. *Nature*, **339**, 721–724.

Madison,E.L., Goldsmith,E.J., Gerard,R.D., Gething,M.-J.H., Sambrook,J.F. and Bassel-Duby,R.S. (1990a) Amino acid residues that affect interaction of tissue-type plasminogen activator with plasminogen activator inhibitor 1. *Proc. Natl Acad. Sci. USA*, **87**, 3530–3533.

Madison,E.L., Goldsmith,E.J., Gething,M.-J.H., Sambrook,J.F. and Gerard,R.D. (1990b) Restoration of serine protease–inhibitor interaction by protein engineering. *J. Biol. Chem.*, **265**, 21423–21426.

Madison,E.L., Kobe,A., Gething,M.J., Sambrook,J.F. and Goldsmith,E.J. (1993) Converting tissue plasminogen activator to a zymogen: a regulatory triad of Asp–His–Ser. *Science*, **262**, 419–421.

Madison,E.L., Coombs,G.S. and Corey,D.R. (1995) Substrate specificity of tissue type plasminogen activator. Characterization of the fibrin independent specificity of t-PA for plasminogen. *J. Biol. Chem.*, **270**, 7558–7562.

Mather,T., Oganessyan,V., Hof,P., Huber,R., Foundling,S., Esmon,C. and Bode,W. (1996) The 2.8 Å crystal structure of Gla-domainless activated protein C. *EMBO J.*, **15**, 6822–6831.

Morgan,P.H., Walsh,K.A. and Neurath,H. (1974) Inactivation of trypsinogen by methane sulfonyl fluoride. *FEBS Lett.*, **41**, 108–110.

Navaza,J. (1994) AMoRe: an automated package for molecular replacement. *Acta Crystallogr.*, **A50**, 157–163.

Nienaber,V.L., Young,S.L., Birktoft,J.J., Higgins,D.L. and Berliner,L.J. (1992) Conformational similarities between one-chain and two-chain tissue plasminogen activator (t-PA): implication to the activation mechanism on one-chain t-PA. *Biochemistry*, **31**, 3852–3861.

Padmanabhan,K., Padmanabhan,K.P., Tulinsky,A., Park,C.H., Bode,W., Huber,R., Blankenship,D.T., Cardin,A.D. and Kisiel,W. (1993) Structure of human des(1–45) factor Xa at 2.2 Å resolution. *J. Mol. Biol.*, **232**, 947–966.

Pannekoek,H., Lijnen,H.R. and Loskutoff,D.J. (1990) Recommendations for the nomenclature of mutant fibrinolytic genes and their proteins. *Thromb. Haemostasis*, **64**, 600–603.

Paoni,N.F., Chow,A.M., Peña,L.C., Keyt,B.A., Zoller,M.J. and Bennett,W.F. (1993a) Making tissue-type plasminogen activator more fibrin specific. *Protein Eng.*, **6**, 529–534.

Paoni,N.F., Keyt,B.A., Refino,C.J., Chow,A.M., Nguyen,H.V., Bereleau,L.T., Badillo,J., Peña,L.C., Bardy,K., Wurm,F.M., Ogez,J. and Bennett,W.F. (1993b) A slow clearing, fibrin-specific, PAI-1 resistant variant of t-PA (T103N, KHRR 296–299 AAAA). *Thromb. Haemostasis*, **70**, 307–312.

Petersen,L.C., Boel,E., Johannessen,M. and Foster,D. (1990) Quenching of the amidolytic activity of one-chain tissue-type plasminogen activator by mutation of lysine-416. *Biochemistry*, **23**, 3451–3457.

Powers,J.C. (1977) Haloketone inhibitors of proteolytic enzymes. In Weinstein,B. (ed.), *Chemistry and Biochemistry of Amino Acids, Peptides and Proteins.* Marcel Decker, New York, pp. 65–178.

Rånby,M., Bergsdorf,N. and Nilsson,T. (1982) Enzymatic properties of the one- and two-chain form of tissue plasminogen activator. *Thromb. Res.*, **27**, 175–183.

Robinson,N.C., Neurath,H. and Walsh,K.A. (1973) Preparation and characterization of guanidinated trypsinogen and ε-guanidinated trypsin. *Biochemistry*, **12**, 414–420.

Silverberg,M. and Kaplan,A.P. (1982) Enzymatic activities of activated and zymogen forms of human Hageman factor (factor XII). *Blood*, **60**, 64–70.

Spraggon,G., Phillips,C., Novak,U.K., Ponting,C.P., Saunders,D., Dobson,C.M., Stuart,D.I. and Jones,E.Y. (1995) The crystal structure of the catalytical domain of human urokinase-type plasminogen activator. *Structure*, **3**, 681–691.

Tachias,K. and Madison,E.L. (1996) Converting tissue type plasminogen activator into a zymogen. *J. Biol. Chem.*, **271**, 28749–28752.

Tachias,K. and Madison,E.L. (1997) Converting tissue type plasminogen activator into a zymogen. Important role of Lys^{156}. *J. Biol. Chem.*, **272**, 28–31.

Tate,K.M., Higgins,D.L., Holmes,W.E., Winkler,M.E., Heyneker,H.L. and Vehar,G.A. (1987) Functional role of proteolytic cleavage at arginine-275 of human tissue plasminogen activator as assessed by site-directed mutagenesis. *Biochemistry*, **26**, 338–343.

Turk,D. (1992) Weiterentwicklung eines Programmes für Molekülgraphik und Elektronendichte Manipulation und seine Anwendung auf verschiedene Protein-Strukturaufklärungen. PhD thesis Technische Universität München.

Wallén,P., Pohl,G., Bersdorf,N., Rånby,M., Ny,M. and Jörnvall,H. (1983) Purification and characterization of melanoma cell plasminogen activator. *Eur. J. Biochem.*, **132**, 681–686.

Wang,D., Bode,W. and Huber,R. (1985) Bovine chymotrypsinogen. A. X-ray crystal structure analysis and refinement of a new crystal form at 1.8 Å resolution. *J. Mol. Biol.*, **185**, 595–624.

Received on April 3, 1997; revised on May 12, 1997